Available online at www.sciencedirect.com

ScienceDirect

Geothermics 00 (2013) 1–8

Geothermics

Feedpoint Viscosity in Geothermal Wellbore Simulation

Mark J. McGuinness

School of Mathematics, Statistics and Operations Research, Victoria University of Wellington, Wellington, New Zealand. Mark.McGuinness@vuw.ac.nz

Abstract

We consider the appropriate way to average reservoir and wellbore viscosities at a feedpoint, when simulating production in a geothermal well. Large differences in these values can arise when flashing occurs in a liquid-dominated reservoir, which may manifest as non-monotonic flowrates in simulated output curves. Integrating Darcy's law for flow to a feed from wellbore to reservoir gives an integral average for the reciprocal of viscosity as a function of pressure that is consistent with the productivity index formulation used in the geothermal wellbore simulators GWELL and SwelFlo. The average is related to the concept of pseudopressure, and various approximations to the integral average are considered, with the result that a trapezoidal rule provides a quick and accurate method. The critical shape of the dependence of average viscosity on wellbore and reservoir pressures is calculated, that separates monotonic from non-monotonic flowrate behaviour, and is found to plot as a straight line. The integral average also reveals that intuition is correct — flow to a feed is monotonic in the pressure there, despite possibly dramatic changes in viscosity.

© 2013 Accepted for publication June 2013

Keywords: Geothermal wellbore simulation, Averaging feed viscosity, Pseudopressure, Flashing in reservoir, GWELL, SwelFlo

1. Introduction

One of the uses of a geothermal wellbore simulator is to compute an output curve, a graph of flowrate versus pressure at the wellhead, for a given wellbore setup. The investigation in this paper was motivated by the observation that when using the simulator GWELL (Aunzo, 1990; Aunzo et al., 1991; Bjornsson, 1987), if the flashpoint crosses the dominant feedpoint, production from the feed and the well can drop despite an increasing pressure difference across the feed, which is counter-intuitive. This behaviour is anticipated from any geothermal wellbore simulator that has too simplistic a treatment of fluid properties at feedpoints.

The problem is illustrated in the output curve in Fig. 1, produced by the geothermal wellbore simulator *SwelFlo* (2013) developed by the author, using the same feed flowrate setup as that in GWELL. The well has one feed at bottomhole. More details on how the well is setup may be found in Appendix B. The output curve is computed by imposing a range of pressure differences across the feed, and integrating up the wellbore to satisfy steady-state conservation of mass, momentum and energy, to find the resulting flow and pressure at the wellhead. Flow into this feedpoint should intuitively be monotonic in the pressure difference between wellbore and reservoir. However, when the flash depth (the transition from liquid to two-phase flow) reaches the bottomhole feed, the change to higher kinematic viscosity in the well due to increased steam content, together with the averaging method used to compute viscosity, sometimes leads to a reduced simulated flowrate despite increasing pressure difference across the feed. This drop in flowrate at the feed is echoed as a drop in the wellhead flowrate, as wellhead pressure drops.

When flow becomes two-phase, variations in relative permeability, density and viscosity in the flow from reservoir to well become important (Grant, 1982). The original coding in GWELL at the well bottom (the lowest feedpoint by definition in the simulator), uses a simple average of wellbore and reservoir densities, relative permeabilities, and dynamic viscosities. The arrival of the flashing front at the feed then leads to an increase in average kinematic viscosity, and a net reduction in flowrate, despite an increase in imposed pressure difference between reservoir and well. This non-monotonic flow behaviour is surprising - what is expected to actually happen is that flowrate increases with pressure drop. We explore the idea here that fluid properties between reservoir and wellbore need to be more carefully treated to ensure this monotonicity.

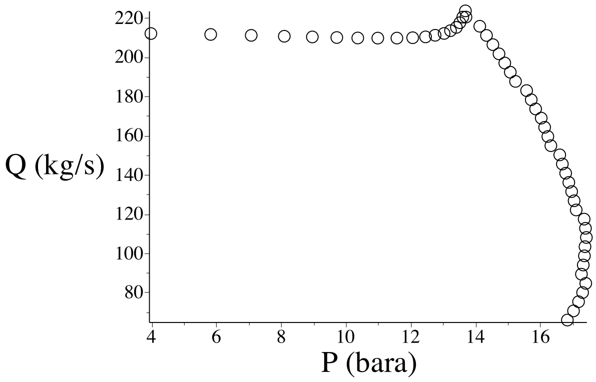

Figure 1. An output curve for a well with a single feedpoint at the bottom, with flowrate on the vertical axis versus wellhead pressure on the horizontal axis. GWELL averages have been used to approximate the viscosity of the fluid at the feed. The output curve shows near a pressure of 14 bara, a counterintuitive reduction in flowrate as wellhead pressure is further reduced. Prior to the reduction, the flash point travels down the wellbore as bottomhole and wellhead pressures decrease. The observed decrease in flowrate at 14 bara coincides with the arrival of the flashing front at the single bottomhole feedpoint, and occurs despite a continually increasing pressure difference between feedpoint and reservoir. The simulator used was *SwelFlo*. More details on the well setup may be found in Appendix B.

In particular, we consider the question of how to most appropriately compute an average value for the viscosity of the flow from reservoir to wellbore, without actually simulating that reservoir flow. We integrate Darcy's law, and we find that the appropriate average to use is an integral average of the reciprocal of two-phase viscosity over the pressure range from well to reservoir.

This integral average has appeared before in the geothermal literature. Tokita and Itoi (2004) present it in their development of the simulator MULFEWS, which is designed to more carefully integrate reservoir flow with wellbore flow. The development here shows further that this treatment of flowrate to a feedpoint has much to recommend it.

The theory is summarised in the next section of this paper. It is then related to the concept of pseudopressure, and a critical linear average viscosity is found that separates monotonic from non-monotonic flows. Then simulated output curves are found to behave consistently with our results.

2. Feedpoint productivity

The usual definition of feedpoint productivity P_1 in the geothermal context is in t/hr/bar,

$$P_1 = \frac{\tilde{Q}}{\left(\tilde{P}_{\text{res}} - \tilde{P}_{\text{well}}\right)}$$

where $\tilde{Q}$ is the flowrate at the feed (t/hr), $\tilde{P}_{\text{res}}$ is reservoir pressure in bars, and $\tilde{P}_{\text{well}}$ is wellbore pressure in bars. An estimate of P_1 is usually determined in a discharge test at given wellbore and reservoir viscosities. When increased production rates are simulated for an output curve, the wellbore viscosity can reduce appreciably, especially if the flashpoint reaches the feedpoint. To allow for changes in viscosity, we rewrite the above equation in the form of Darcy's law for flow, as

$$Q = \frac{\Sigma}{\nu}\,(P_{\text{res}} - P_{\text{well}}) \tag{1}$$

where the number Σ is called a *productivity index* (units m^3), ν is the kinematic viscosity ($m^2.s^{-1}$), and flowrate and pressures are now in kg/s and Pa. This productivity index is related to the more usual productivity P_1 by:

$$\Sigma = \frac{P_1\,\nu_1}{3.6 \times 10^5}\,.$$

Usually P_1 is estimated from, and valid for, just one set of known flow conditions from a discharge test, which give ν_1, and then it is desired to use it to obtain an output curve. The best way to calculate the output curve is to estimate a value for the productivity index Σ from the given value of P_1. This is then used in equation (1) to calculate the flows Q at a feedpoint, given various pressures in the wellbore. This approach properly accounts for the effects of changes in viscosity on feed flowrate — the productivity index Σ is independent of these.

This method for determining the productivity of a feedpoint by using a productivity index Σ is used in the wellbore simulators GWELL (Aunzo, 1990; Aunzo et al., 1991; Bjornsson, 1987) and *SwelFlo* (2013).

This formulation is straightforward to apply when ν is roughly the same in the reservoir and in the wellbore. When ν varies significantly between well and reservoir pressures, as it does when flow becomes two-phase in the reservoir, some care is needed in calculating an effective average value of ν.

Equation (1) can be written in terms of varying $\nu(P)$, with a pressure gradient dP/dr across a surface at pressure P, in the form of Darcy's law (Nield and Bejan, 1998),

$$W = -\frac{kA}{\nu(P)}\frac{dP}{dr}\,, \tag{2}$$

where k is an effective permeability of the surface to flow, W is the mass flow rate (positive if flowing outwards from the well to the reservoir), r is distance from the well, and A is the cross-sectional area of the surface normal to the flow. Furthermore, ν is in general the two-phase kinematic viscosity,

$$\frac{1}{\nu} = \frac{k_{rl}}{\nu_l} + \frac{k_{rv}}{\nu_v}\,,$$

where $k_{rl} = 1 - S$ and $k_{rv} = S$ are relative permeabilities for liquid and steam, respectively; S is steam saturation; and ν_l and ν_v are kinematic viscosities for liquid and steam phases of water, respectively.

Rearranging this, and using $Q = -W$ so that positive Q corresponds to production, and integrating with respect to distance r from origin at the centre of the wellbore to undisturbed reservoir at a distance R in a one-dimensional reservoir with constant area A gives

$$\int_0^R Q dr = kA \int_0^{P_{\rm res}} \frac{dP}{\nu(P)} \, . \tag{3}$$

Hence

$$Q = \frac{kA}{R} \int_0^{P_{\rm res}} \frac{dP}{\nu(P)} \, , \tag{4}$$

and this can be written in the desired form $Q = \frac{\Sigma}{\nu_{\rm eff}} (P_{\rm res} - P_{\rm well})$ provided that $\Sigma = \frac{kA}{R}$, and

$$\frac{1}{\nu_{\rm eff}} = \left(\frac{1}{P_{\rm res} - P_{\rm well}} \right) \int_{P_{\rm well}}^{P_{\rm res}} \frac{dP}{\nu(P)} \, . \tag{5}$$

This is the integral average value of $1/\nu$ when plotted against pressure, so that areas under curves match, as illustrated in Fig. 2. The value for effective viscosity for flow to the feedpoint that is most consistent with Darcy's law will be obtained by calculating numerically the integral above. Note that when flow is single phase, and/or the kinematic viscosity is practically constant, this formulation drops back to the simple case (1). The integral average of the reciprocal of viscosity provides a smooth combination of both single and two-phase flow conditions.

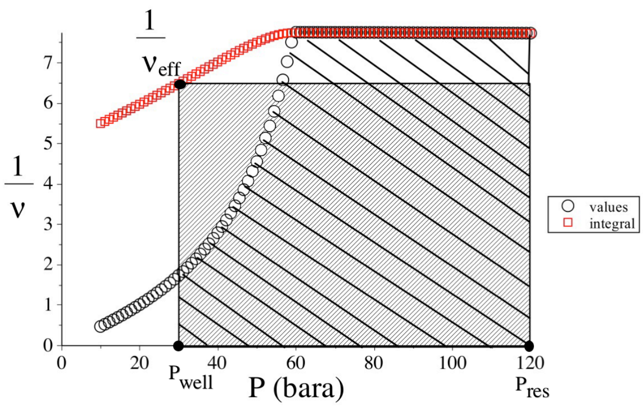

Figure 2. An illustration of the reciprocal of the effective viscosity. The black circles show the way that reciprocal two-phase viscosity varies with pressure, for a fluid with enthalpy 1200 kJ/kg. The shaded area under these between 30 and 120 bara, matches the finely shaded area under the value $1/\nu_{\rm eff}$ at 30 bara. $1/\nu_{\rm eff}$ is then an integral average of the reciprocal of viscosity, over the given pressure range, and is given by the red squares. Values of $1/\nu$ were calculated in units of m^{-2}.s, and have then been multiplied by 10^{-6} before plotting.

This integral average is essentially the same as the formulation presented by Tokita and Itoi (2004) for their MULFEWS simulator, where they study the role of a feedpoint as the interface between flow in the reservoir and flow in the well.

Also note that integrating Darcy's law for other reservoir geometries, cylindrical and spherical with radial symmetry, also leads to the same integral average of reciprocal viscosity. See Appendix A for details.

2.1. Pseudopressure

The integral average appearing in eqn. (5) may be further interpreted by considering the quasi-steady equation for isothermal gas flow in a porous medium (Grant, 1982, p.293)

$$\nabla \left(\frac{k}{\nu} \nabla P \right) = 0 \, . \tag{6}$$

This can be rewritten as

$$\nabla^2 m = 0 \tag{7}$$

where the pseudopressure $m(P)$ is defined to be

$$m \equiv \int \frac{1}{\nu} \, dP \, .$$

So the integral average of reciprocal viscosity is related to the pseudopressure concept in a steam-dominated reservoir.

2.2. Approximating Pseudopressure

The simplest approximation to $1/\nu_{\rm eff}$ would be the usual arithmetic average of $1/\nu$, using reservoir and wellbore values, that is

$$\frac{1}{\nu_{\rm eff}^{(1)}} = \frac{1}{2} \left(\frac{1}{\nu_{\rm well}} + \frac{1}{\nu_{\rm res}} \right) \, . \tag{8}$$

This will be an underestimate of $1/\nu_{\rm eff}$, that is, will give values of viscosity that are too large, as illustrated in Fig. 3.

A consideration of the shape of the graph of $1/\nu$ versus pressure as plotted in Fig. 3 shows that a better approximation if flashing occurs in the reservoir, is to compute the pressure $P_{\rm flash}$ at which flashing occurs, and then to take the more sophisticated weighted average that results from adding the areas, one between $P_{\rm flash}$ and $P_{\rm res}$ assuming it is a rectangle, and one between $P_{\rm well}$ and $P_{\rm flash}$, assuming it is a single trapezoid, to get the formula

$$\frac{1}{\nu_{\rm eff}^{(2)}} = \frac{\frac{1}{\nu_{\rm res}} (2P_{\rm res} - P_{\rm flash} - P_{\rm well}) + \frac{1}{\nu_{\rm well}} (P_{\rm flash} - P_{\rm well})}{2\,(P_{\rm res} - P_{\rm well})} \, . \tag{9}$$

The average that is used at bottomhole in GWELL bears no resemblance to any of the above approximations in formulation, but does give numerical values that are seen in Fig. 3 to be similar to the simple average $1/\nu_{\rm eff}^{(1)}$. An average saturation $\bar{S} = (S_{\rm well} + S_{\rm res})/2$ is used to find average relative permeabilities $\bar{k}_{rl} = 1 - \bar{S}$ and $\bar{k}_{rv} = \bar{S}$; an average vapour $\bar{\rho}_v$ and liquid density $\bar{\rho}_l$ is calculated similarly; an average dynamic liquid $\bar{\mu}_l$ and vapour viscosity $\bar{\mu}_v$ is calculated; then the average kinematic viscosity is taken in GWELL as

$$\frac{1}{\bar{\nu}} = \frac{\bar{k}_{rl} \bar{\rho}_l}{\bar{\mu}_l} + \frac{\bar{k}_{rv} \bar{\rho}_v}{\bar{\mu}_v} \, . \tag{10}$$

Note that a twenty-point trapezoidal method for finding the area under the curve is graphically indistinguishable from the accurate integration method in Fig. 3. We will call the resulting average effective viscosity $\nu_{\rm eff}^{(3)}$. Given the simplicity of implementation, this is the method recommended here for using in geothermal reservoir simulators.

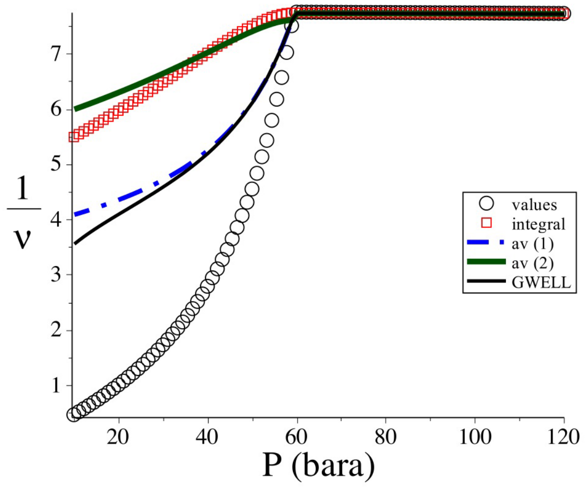

Figure 3. Comparisons of different average reciprocals of effective viscosities. The black circles show the actual values of $1/\nu$ (m^{-2}.s, multiplied by 10^{-6}) at each value of pressure. Average values of $1/\nu$ must start at some pressure, which is here taken to be a reservoir pressure of 120 bara for illustration purposes. For averages, the wellbore pressure is the P-coordinate of the value plotted. The correct integral average of the circles, the value with an area matching that under the curve between the current P value and the value 120 bara, is given by the red squares. These accurate values for the integral were calculated by using an automatic Gauss-Kronrod integrator, with relative global error set to 0.1%. The three approximations shown are the simple average $1/\nu_{\text{eff}}^{(1)}$ labelled (1), the more careful average $1/\nu_{\text{eff}}^{(2)}$ labelled (2), which gives a reasonably close match to the accurate integral average, and the GWELL average, which gives values similar to $1/\nu_{\text{eff}}^{(1)}$. A simple twenty-point trapezoidal rule numerical integration gave values that could not be distinguished graphically from the accurate Gauss-Kronrod integrator (red squares). Fluid enthalpy is fixed at 1200 kJ/kg, flashing at about 60 bara. Carbon dioxide is set to 0.1 weight % .

A comparison of the output curves that can be obtained, when simulating production from a geothermal well with *SwelFlo* using this original GWELL average viscosity, the simple approximation $\nu_{\text{eff}}^{(1)}$, and the more accurate trapezoidal $\nu_{\text{eff}}^{(3)}$, is presented in Fig. 4. Note that the use of the more accurate average is successful in ensuring that flowrate remains monotonic with reducing wellbore pressure, through values where the flashpoint reaches the feed. The wellbore geometry and feed properties are outlined in detail in Appendix B.

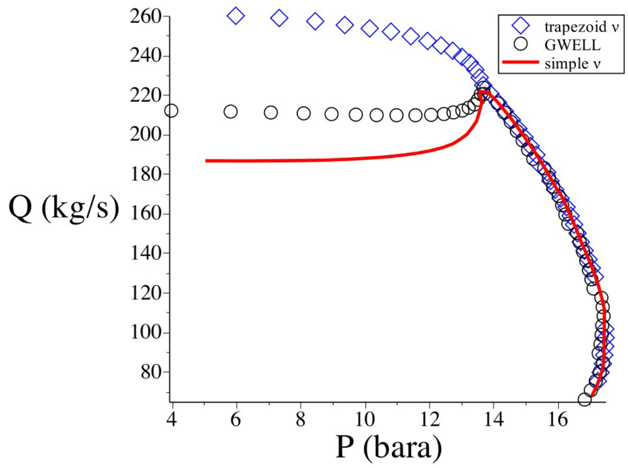

Figure 4. Simulated output curves for a well with a single feedpoint at the bottom, with flowrate on the vertical axis versus wellhead pressure on the horizontal axis. The effect of using different averages to approximate the viscosity of the fluid at the feed is illustrated. The output curves are different past the arrival of the flashing front at the single bottomhole feedpoint, at about 13 bara wellhead pressure, and 220 kg/s flowrate. The simple approximation $\nu_{\text{eff}}^{(1)}$ and the GWELL average both exhibit a non-monotonic dependence of flowrate on wellhead pressure, due to increased average feed viscosity. The more accurate trapezoidal average $\nu_{\text{eff}}^{(3)}$ gives a monotonic increasing flowrate at the feed, with increasing pressure differences driving the flow. The simulator used was *SwelFlo* (2013). More details on the well setup may be found in Appendix B.

2.3. *Critical average viscosity*

One question that arises in this work is what is the critical slope of average inverse viscosity at which the flowrate fails to be monotonic in wellbore pressure. GWELL and the simple average have steep $1/\nu$ slopes that lead to non-monotonic flowrates, while the more accurate integral averages have gentler slopes and lead to monotonic curves.

That is, when is the area sketched in Fig. 5, equal to $\frac{P_{\text{res}}-P_{\text{f}}}{\nu_0}$, where P_{f} is the flash pressure? This happens when

$$\frac{P_{\text{res}} - P_{\text{f}}}{\nu_0} = \frac{P_{\text{res}} - P_{\text{well}}}{\nu_c} .$$

This equation may be rearranged to find the critical value ν_c

$$\nu_c = \nu_0 \left(\frac{P_{\text{res}} - P_{\text{well}}}{P_{\text{res}} - P_{\text{f}}} \right) .$$

This gives a straight line if ν_c is plotted against P_{well}, as illustrated together with the various approximations discussed earlier replotted as ν versus P_{well} in Fig. 6. This value of average ν

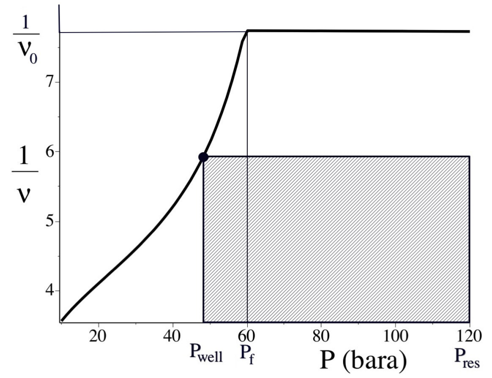

Figure 5. A sketch showing the area that corresponds to the value of $\frac{P_{res}-P_{well}}{\nu}$ and the graph of $1/\nu$ versus P_{well}, when $P_{res} = 120$. The $1/\nu$ curve used for illustration purposes here is the GWELL average. The $1/\nu$ axis is in m^{-2}.s, after it is multiplied by 10^{-6}.

would give a constant flowrate as P_{well} drops below flash value. Average values of ν graphing above this line, such as the simple average and the GWELL average, will give non-monotonic flowrate behaviour, while values graphing below this critical line give monotonic flowrates that continue to increase with pressure differences across the feedpoint.

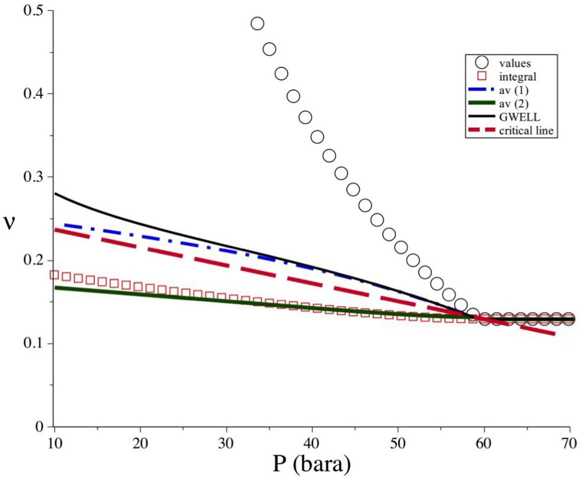

Figure 6. Values of ν times 10^6 (m^2.s^{-1}) versus pressure. The black circles are actual viscosity values at the pressure given, while the other values are averages as detailed in the text and in Fig. 3. The averages are taken between the pressure given and the reservoir pressure $P_{res} = 120$. The three approximations shown are the simple average $\nu_{\text{eff}}^{(1)}$ labelled (1), the more careful average $\nu_{\text{eff}}^{(2)}$ labelled (2), which gives a reasonably close match to the accurate integral average (red squares), and the GWELL average. The dashed red line shows the critical value ν_c, below which the average will give a monotonic flowrate as wellbore pressure is decreased further. Enthalpy is 1200 kJ/kg. Flash pressure is about 60 bara.

Note that the slope of this straight line may be easily changed in a simulation, by changing the value of reservoir pressure. Making this pressure larger will reduce the slope, and may hence reveal non-monotonic flowrate behaviour if a simple enough average has been used at the feed. Conversely, even when using the GWELL average viscosity, reducing the pressure difference to 4 bars for example causes monotonic behaviour. Getting reasonable flowrates from such a small pressure difference would require a very productive feedpoint.

3. Conclusions

An improved method for computing the average two-phase viscosity at a feedpoint is derived by integrating Darcy's law. This average is more likely to give a feed flowrate that is monotonic in wellbore pressure, during the process of generating an output curve with a geothermal wellbore simulator. This improved average is an integral average of the reciprocal of viscosity as a function of pressure, so that flow at a feedpoint is given by the formula

$$Q = \frac{\Sigma}{\nu_{\text{eff}}} (P_{\text{res}} - P_{\text{well}})$$

where Σ (m^3) is a productivity index, and the effective reciprocal two-phase viscosity is

$$\frac{1}{\nu_{\text{eff}}} = \left(\frac{1}{P_{\text{res}} - P_{\text{well}}}\right) \int_{P_{\text{well}}}^{P_{\text{res}}} \frac{dP}{\nu(P)} ,$$

and is related to the concept of pseudopressure in a gas reservoir.

We find that a twenty-point trapezoidal rule is accurate enough to ensure monotonic dependence of feed flowrate on drawdown, whereas simple two-point averages may not be, depending on the pressure difference across the feedpoint. We also derive a formula for the critical dependence of average feed viscosity on pressures at the feed and in the reservoir, above which the output curve will be non-monotonic if flashing moves from wellbore to reservoir, while generating an output curve.

This study also answers the question, should the flowrate to a feedpoint be monotonic in wellbore pressure there? That is, is it possible that a reduction in feedpoint flowrate could result from increased viscosity near the wellbore, despite the increase in pressure drop that is causing the increased viscosity? The formula

$$Q = \frac{kA}{f(R)} \int_{P_{\text{well}}}^{P_{\text{res}}} \frac{dP}{\nu(P)} ,$$

where $f(R)$ is a geometric term that depends on the wellbore radius, the reservoir radius and the reservoir geometry, reveals the answer — Q is monotonic in P_{well}, since ν takes only positive values. Another way to see this is that the rate of change of Q with P_{well} is, by differentiating the above equation and using the Fundamental Theorem of Calculus,

$$\frac{dQ}{dP_{\text{well}}} = -\frac{kA}{f(R)} \frac{1}{\nu(P_{\text{well}})}$$

which is clearly always negative, so that reduced wellbore pressures should give increased flowrates.

Acknowledgements

This work arose directly out of discussions with Dr. Malcolm Grant a number of years ago. Dr. Grant noticed non-monotonic behaviour during output curve simulations, and it was his suggestion to try a pseudopressure approach.

References

Aunzo, Z.P., 1990. GWELL : a multi-component multi-feedzone geothermal wellbore simulator. M.S. Thesis, University of California, Berkeley. 250 pp.

Aunzo, Z.P., Bjornsson, G., Bodvarsson, G., 1991. Wellbore models GWELL, GWNACL, and HOLA User's Guide. Lawrence Berkeley Lab, University of California, Earth Sciences Division Report LBL-31428, UC-251. 103pp.

Bjornsson, G., 1987. A multi-feed zone wellbore simulator. Masters Thesis, University of California, Berkeley. 102 pp.

Grant, M.A., Donaldson, I.G., Bixley, P.F., *Geothermal Reservoir Engineering*, Academic Press, 1982. 369 pp.

Nield, D.A., Bejan, A., *Convection in Porous Media*, Springer-Verlag, NY, 1998. 546 pp.

SwelFlo is a geothermal wellbore simulator developed by the author. It was originally based on GWELL, but is extensively modified and rewritten in Fortran 90, and is blended with a GUI to run under the Microsoft Windows environment.

Tokita, H., Itoi, R, 2004. Development of the Mulfews multi-feed wellbore simulator. *Proc 29th Workshop on Geothermal Reservoir Engineering, Stanford University*, Stanford, California, January 26-28, 2004. 9 pp. SGP-TR-175

Appendix A. Radial Symmetry

Here we show that our simple linear development extends to cylindrical and spherical geometries with radial symmetry.

Appendix A.1. Cylindrical Geometry

In cylindrical geometry with radial symmetry, Darcy's law for the flow inwards (kg/s) across the curved surface of a cylinder of height h at a distance r from the centre of a well is

$$Q = \left(\frac{2\pi rkh}{\nu}\right)\frac{\partial P}{\partial r} .$$

This rearranges to

$$\frac{Q}{r} = \frac{2\pi kh}{\nu}\frac{\partial P}{\partial r}$$

and integrating both sides with respect to r from wellbore value R_{well} to reservoir value R_{res} gives

$$\int_{R_{\text{well}}}^{R_{\text{res}}} \frac{Q}{r}\, dr = \int_{R_{\text{well}}}^{R_{\text{res}}} \frac{2\pi kh}{\nu}\frac{\partial P}{\partial r}\, dr = 2\pi kh \int_{P_{\text{well}}}^{P_{\text{res}}} \frac{dP}{\nu(P)}$$

assuming constant k and h, and assuming P is steady-state and depends only on r. That is, evaluating the left-hand side and rearranging,

$$Q = \left(\frac{2\pi kh}{\ln(R_{\text{res}}/R_{\text{well}})}\right)\int_{P_{\text{well}}}^{P_{res}} \frac{dP}{\nu(P)} .$$

This takes the form used in simulations

$$Q = \frac{\Sigma}{\nu_{\text{eff}}}\,(P_{\text{res}} - P_{\text{well}})$$

provided that

$$\Sigma = \left(\frac{2\pi kh}{\ln(R_{\text{res}}/R_{\text{well}})}\right)$$

and

$$\frac{1}{\nu_{\text{eff}}} = \left(\frac{1}{P_{\text{res}} - P_{\text{well}}}\right)\int_{P_{\text{well}}}^{P_{\text{res}}} \frac{dP}{\nu(P)} .$$

Appendix A.2. Spherical Geometry

In spherical geometry with radial symmetry, Darcy's law for the flow inwards (kg/s) across the curved surface of a sphere at a distance r from the centre of a feed is

$$Q = \left(\frac{4\pi r^2 k}{\nu}\right)\frac{\partial P}{\partial r} .$$

This rearranges to give, after integrating both sides with respect to r from wellbore to reservoir in a similar approach to the previous subsection:

$$Q = \left(\frac{4\pi k}{1/R_{\text{well}} - 1/R_{\text{res}}}\right)\int_{P_{\text{well}}}^{P_{res}} \frac{dP}{\nu(P)} .$$

This takes the form

$$Q = \frac{\Sigma}{\nu_{\text{eff}}}\,(P_{\text{res}} - P_{\text{well}})$$

provided that

$$\Sigma = \left(\frac{4\pi k}{1/R_{\text{well}} - 1/R_{\text{res}}}\right)$$

and

$$\frac{1}{\nu_{\text{eff}}} = \left(\frac{1}{P_{\text{res}} - P_{\text{well}}}\right)\int_{P_{\text{well}}}^{P_{\text{res}}} \frac{dP}{\nu(P)} .$$

Appendix B. Wellbore Simulation Details

The wellbore simulations used to illustrate the effects of feed viscosity treatment were done with *SwelFlo*, a multiple feed-point geothermal wellbore simulator developed by the author that allows topdown and bottom up steady-state simulations of two-phase flow of water and noncondensible gas, up a wellbore of varying radius, roughness and inclination angle. The generic well setup was a vertical well 2000m long, cased to 900m with casing of 0.16m radius and roughness 4.6×10^{-5}m, then with liner of 0.125m radius and 4.6×10^{-4}m. No heat transfer to or from the surrounding country was allowed. The reservoir fluid supplying the feed at bottomhole had 0.1% CO_2 by weight, was at a pressure of 140 bara, and an enthalpy of 1200 kJ/kg. The productivity index used was 10^{-12}m^3. Computations up the wellbore used a mesh size of 20m, with reduction to 1m to more accurately find the flash depth when it occurs in the well.